Leading-Edge-Vortex Augmentation in Compressible Flow

R.G. Bradley,* P.D. Whitten,† and W.O. Wray†
General Dynamics, Fort Worth, Texas

Leading-edge-vortex enhancement by blowing has been explored experimentally. Conceptual half-span wind-tunnel tests were conducted on a wing-body-tail configuration with a cambered and twisted wing with leading-edge flaps. Blowing vortex augmentation is shown to be effective in improving both lift and drag due to lift at high angle of attack for the Mach numbers tested, $M=0.3$ and 0.75. Drag improvement results, in part, from an apparent vortex-suction effect on the cambered wing.

Nomenclature

c	= local wing chord
C_D	= drag coefficient
C_L	= lift coefficient
C_{L0}	= lift coefficient for $C_\mu = 0$
C_M	= moment coefficient about ¼ mac
C_μ	= momentum coefficient
$(x/c)_N$	= nozzle chordwise position
α	= angle of attack
δ_{LE}	= leading-edge-flap deflection
Λ_N	= nozzle sweep

Introduction

THE concept of leading-edge-vortex enhancement by blowing has been demonstrated to hold promise for improvement of lift and drag for advanced aircraft (Refs. 1-3, for example). Blowing a stream of high-pressure air in the leading-edge-vortex axial direction aids in the formation of the vortex for wings with low leading-edge sweep and intensifies the natural vortex flow that exists for wings of high sweep. Vortex burst is delayed to higher angles of attack by blowing.

Cornish[1] was among the first to point out the potential of vortex augmentation by spanwise blowing, and Werle[2] has published flow-visualization studies of the vortex augmentation. Bradley and Wray, in Ref. 3, demonstrated for a series of low-aspect-ratio flat-plate wings that leading-edge-vortex augmentation significantly increases the aerodynamic efficiency for wings at high angle of attack. It is further shown in Ref. 3 that the vortex-lift increments obtained with spanwise blowing approach the level predicted by the Polhamus[4] leading-edge-suction analogy theory. Dixon, et al.[5] have conducted recent experimental studies on the effects of blowing, and have explored some of the theoretical principles underlying the vortex formation over the wing surface. Reference 6 presents a NASA sponsored experimental study of wing-body configurations with vortex enhancement for a family of arrow, diamond, and delta wings.

Most all of the work done to data has dealt with low-speed flows. Emphasis at General Dynamics has been placed on the application of the concept to fighter aircraft for maneuver enhancement. This paper presents the result of some conceptual experimental investigations designed to explore the aerodynamic effects of vortex augmentation on a research configuration with emphasis on the higher subsonic Mach regime. The configuration features a cambered and twisted wing, and the studies include the effect of vortex enhancement in conjunction with deflected leading-edge flaps.

Presented as Paper 75-124 at the AIAA 13th Aerospace Sciences Meeting, Pasadena, Calif. Jan. 20-22, 1975; submitted Jan. 27, 1975; revision received June 16, 1975.

Index Categories: Aircraft Aerodynamics (including Component Aerodynamics); Subsonic and Transonic Flow.

*Design Specialist, Aerospace Technology Department. Associate Fellow AIAA.

†Senior Aerodynamics Engineer, Aerospace Technology Department.

Wind-Tunnel Test

Test Facilities

Force tests and limited smoke flow-visualization studies were conducted with a half-span research model. Figure 1 shows a schematic layout of the free jet wind tunnel used for force testing. A reflection plane surface located at the exit of a 9.75-in. square duct is used for mounting the half-span research model. Ambient air is drawn through a large bellmouth inlet and then merged into the duct section. The duct exits into a large plenum chamber, which is connected to an ejector system. Pressure orifices located near the duct exit are utilized to determine the freestream velocity for the free-jet flow.

Model and Instrumentation

The model that was tested is a half-span, small-scale research model of an advanced fighter configuration with a faired-over inlet. The fuselage length was 10.3 in. Pertinent wing parameters are shown in Table 1.

A photograph of the half-span model mounted on the reflection plane is shown in Fig. 2. The reflection plane surface was used to support a three-component moment-type balance for force measurements and to position the convergent nozzle for directing air over the model surface. High-pressure air for vortex augmentation was supplied through a 0.060-in.-diam convergent nozzle mounted to the reflection plate. Only the model was attached to the balance, so that the measured forces are the aerodynamic forces acting on the configuration and do not include the nozzle thrust components. The air supply tube was extended through the model fuselage to its position above the wing, as shown in Fig. 2. A small open space around the tube was maintained to prevent interference between the tube and the model due to balance and/or model deflection under load.

A wide range of nozzle positions were made available by chordwise positioning and by bending the nozzle tubing. The range of positions are illustrated in Fig. 3. The versatility in nozzle positioning was considered to be more important for the present conceptual tests than a high degree of precision in measurement of the position. In all cases, the nozzle vertical

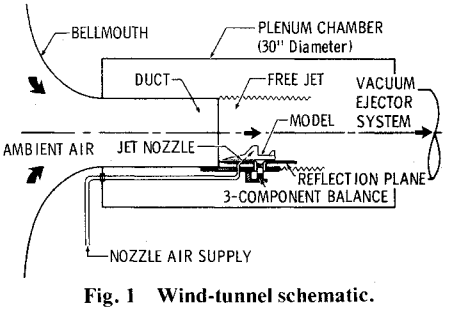

Fig. 1 Wind-tunnel schematic.

Table 1 Wing parameters

Aspect ratio, $\mathcal{R}$	3.173
Taper ratio, λ	0.200
Sweep, Λ_{LE}	40°
Section	NACA 64A204
Aerodynamic twist	3°

position was approximately one nozzle diameter above the wing surface, although precise control was most difficult because of model/balance deflection, especially at the highest Mach numbers.

Force Tests

Force and moment data were taken for nominal Mach numbers of 0.3 and 0.75 and Reynolds number per foot of 1.8 and 4.0 million, respectively. Data were taken over a pitch range of from 0° to 30°. Momentum coefficient C_μ is defined as $\dot{m}V_j/q_\infty S$, where $\dot{m}$ is the mass flow rate and V_j is the fully expanded isentropic jet velocity. C_μ was varied from zero to the value corresponding to a supply total pressure of approximately 300 psia ($C_\mu \simeq 0.17$ at $M=0.3$ and $C_{5\mu} \simeq 0.038$ at $M=0.75$). The major emphasis of the test was on the higher Mach number range, so that most of the data were taken at $M=0.75$, the highest value that could be consistently attained in the 0.75-in. square free-jet section. Configuration variations included, leading-edge flap deflections of 0°, 10°, and 25°.

As a result of the combined effects of the reflection-plane technique and the free-jet tunnel, the lift-curve slope is expected to be somewhat lower (on the order of 10%) than would be expected for a full model in free air. No corrections to the data were made for either half-span or free-jet effects. However, the objectives of this conceptual test are not impaired by the slightly reduced lift forces of the semispan model, since the relative leading-edge-vortex-enhancement effects due to blowing are clearly evident.

Results and Discussion

Low-Speed Test Results

Systematic low-speed data were taken only the the zero leading-edge-flap configuration. A summary of the effects of blowing on the lift, drag, and pitching moment is presented in Fig. 4, where momentum coefficient C_μ varies from 0 to 0.17. The data shown represent the nozzle position, giving the greatest lift increment of those tested for each angle of attack. A discussion of the nozzle position studies is given in a later section. Very large improvements in lift and drag are evident in the figure, especially at the higher blowing rates. The characteristic nonlinearity in the lift curve that results from vortex augmentation and the improved drag-polar shape are noted. A further effect of vortex augmentation is noted to extend the moment curve to higher angles of attack without adverse pitchup characteristics.

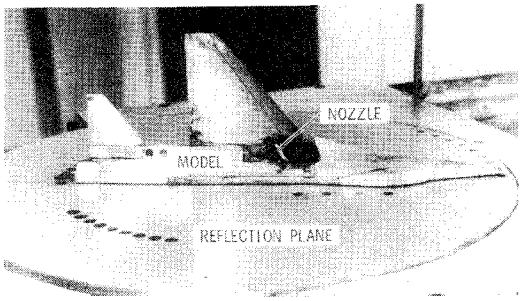

Fig. 2 Half-span model.

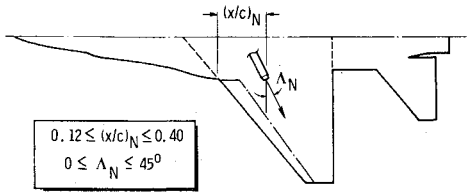

Fig. 3 Nozzle position schematic.

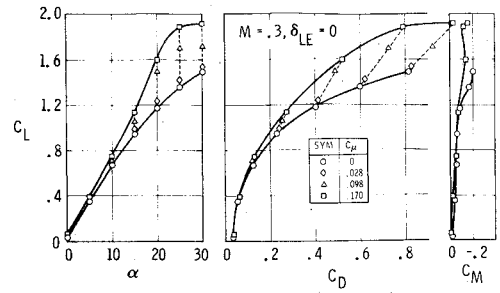

Fig. 4 Low-speed blowing effect.

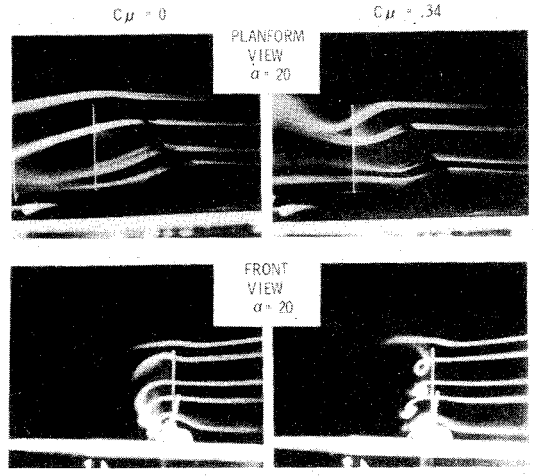

Fig. 5 Smoke flow visualization.

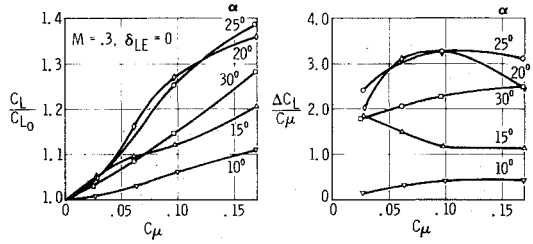

Fig. 6 Low-speed lift effectiveness.

Figure 6 illustrates the lift effectiveness of the vortex augmentation scheme. The curves on the left give a measure of the lift gains in the form of the ratio of lift with blowing to the lift without blowing as a function of momentum coefficient C_μ. Gains of well over 30% in lift are apparent at higher values of momentum coefficient. The right-hand plot relates the generated lift increment to the added lift that could be achieved by simply directing the jet downward in a direction perpendicular to the freestream. One notes that, at angles of attack of 20° and above, the vortex lift generated is two to

The qualitative effects of the blowing on the wing upper-surface flowfield is shown in Fig. 5. The left-hand smoke flow photographs show clearly the separated flowfield above the wing without blowing. The right-hand photographs reveal that with blowing the flowfield is altered dramatically. A stronger vortex forms along the leading edge and the flow reattaches to the wing aft of the vortex. The result is the rather large component of vortex lift, as noted in the force data shown in Fig. 4. The large value of momentum coefficient C_μ for the smoke flow visualization studies is a result of the very low freestream dynamic pressure of the smoke tunnel tests. These flowfield photographs do illustrate, however, the flow phenomena that occur throughout the C_μ range.

three times the ideal thrust of the nozzle for the C_μ range tested.

The augmented vortex flow has a pronounced effect on the drag polar shape, especially at the higher angles of attack. This polar improvement is evidenced in Fig. 4. For a thin wing with a sharp leading edge, the improvement in the drag polar shape is a result of the improvement in the lift curve and its effect on the zero-suction, drag-due-to-lift increment, $\Delta C_L \tan\alpha$. This drag effect was apparent in previous comparisons of flat-plate-wing lift and drag test data, with predictions obtained from the Polhamus zero-suction, drag-due-to-lift method, given in Ref. 3.

The polar improvement in the present case, however, benefits in part from an increase in suction forces on the cambered wing surface, since it is influenced by the augmented wing vortex system. The drag improvement relative to the zero-suction drag due to lift is visible in Fig. 7, where the measured drag increment due to blowing is plotted against the zero-suction drag-due-to-lift increment at constant alpha. Drag savings on the order of 20% over the zero-suction increment are noted. These results suggest that good polar improvements may be possible if the upper surface of the wing is contoured to take advantage of the enhanced vortex. There exists, then, the rather exciting possibility for designing a wing to take advantage of the separated upper-surface flow, rather than attempting to maintain attached flow at high angles of attack.

High-Speed Test Results

No Flap Deflection

The effect of vortex augmentation on forces and moments at 0.75 Mach number is summarized in Fig. 8. The nozzle locations again are those giving the best lift increment of those tested for each angle of attack. note that the momentum coefficient range is significantly less than for the $M=0.3$ condition as a result of the higher freestream dynamic pressure for $M=0.75$.

The favorable effects of vortex augmentation on the lift and drag are clearly evident in Fig. 8 for $\delta_{LE}=0$. The effects are much less dramatic than those in low-speed case; this is the result of the reduced C_μ. As a matter of fact, one of the great deterrents to applying the blowing concept at transonic Mach numbers is that engine bleed air may not be readily available to supply the momentum required for effective vortex augmentation.

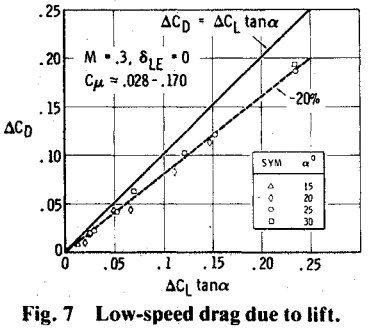

Fig. 7 Low-speed drag due to lift.

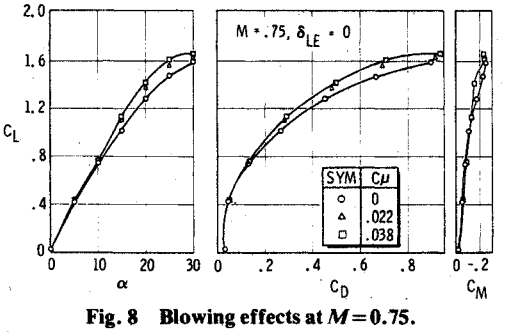

Fig. 8 Blowing effects at $M=0.75$.

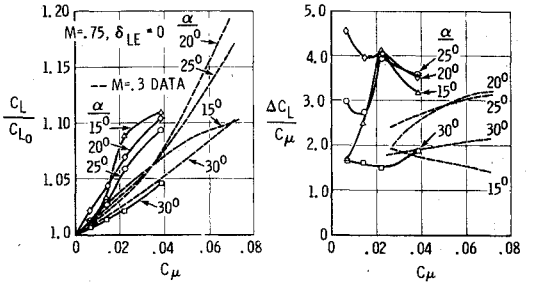

Fig. 9 Lift effectiveness at $M=0.75$.

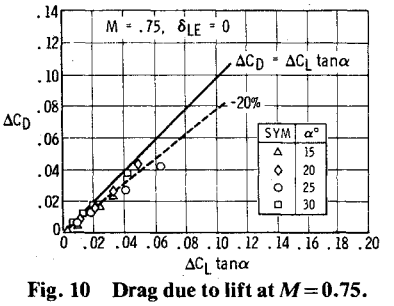

Fig. 10 Drag due to lift at $M=0.75$.

The lift effectiveness for high subsonic speed flow is presented in Fig. 9. As in the low-speed case, the left-hand figure shows the ratio of lift with blowing to that without blowing as a function of C_μ. For comparison, data from the low-speed plot (Fig. 6) also are shown on the figure for the C_μ range of the high-speed tests. At $M=0.75$, blowing is noted to be generally more effective than comparable blowing rates for the $M=0.3$ case. The same conclusion may be drawn from the right-hand plot, where the lift increment due to blowing divided by the momentum coefficient is plotted. Blowing ratios of 3 to 4 were noted to be possible over the angle-of-attack range of 15° to 25°. These results show that vortex augmentation is effective at high subsonic Mach numbers, thus lending support to the idea of using vortex augmentation to supplement the maneuver capability of fighter aircraft.

The measured drag increment is compared to the zero-suction drag due to lift, $\Delta C_L \tan\alpha$, in Fig. 10. As in the low-speed case, the drag increments are significantly below the flat-plate level, indicating that a measurable leading-edge thrust results from the augmented vortex flow. In evaluating the drag improvement for both low speed and high speed it should be kept in mind that these data contain only aerodynamic forces, and no thrust force components are measured. Of course, the true benefit for fighter application must measure the increased lift and improved drag against the thrust lost required to duct and jet the high-momentum air over the wing upper surface. In this bookkeeping system, the component of nozzle thrust also must be taken into account.

With Flap Deflection

The effectiveness of blowing vortex augmentation, when combined with deflected leading-edge flaps, is shown in Figs. 11 and 12. For leading-edge deflections of 10° and 25°, leading-edge-vortex augmentation becomes effective when the wing upper-surface flow is separated from, or near, the leading edge. Deflected leading-edge flaps tend to maintain attached wing flow to higher angles of attack. Thus, one would expect the favorable effect of blowing to be seen at higher angles of attack when the leading-edge flap is deflected. This effect is illustrated clearly when one compares Figs. 8, 11, and 12, representing leading-edge flap deflections of 0°, 10°, and 25°, respectively. At 25° deflection, blowing is not at all effective below an angle of attack of about 20°. As long as the leading-edge flap is effective in maintaining an attached leading-edge flow, the spanwise blowing has little effectiveness. However, as an angle of attack is reached where the leading edge stalls, either at the leading edge or perhaps at

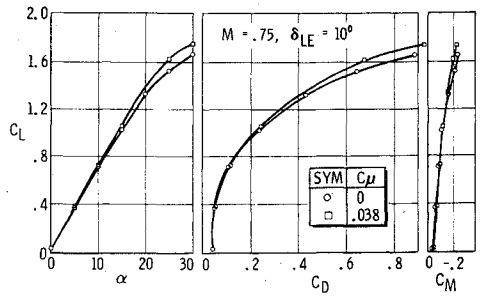

Fig. 11 Leading-edge-flap effect, δ_{LE} 10°.

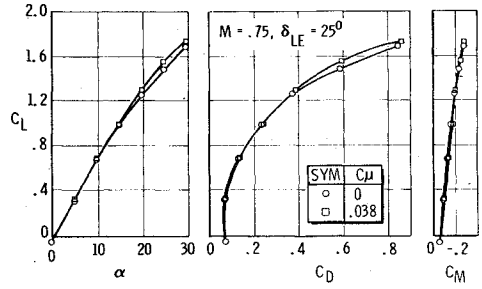

Fig. 12 Leading-edge-flap effect, $\delta_{LE} = 25°$.

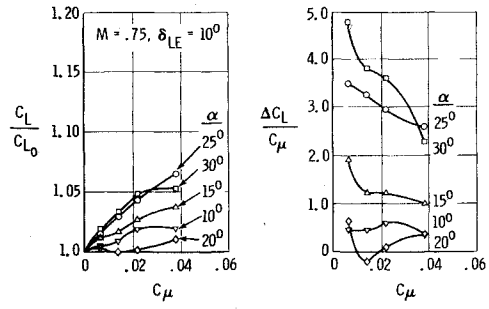

Fig. 13 Lift effectiveness, $\delta_{LE} = 10°$.

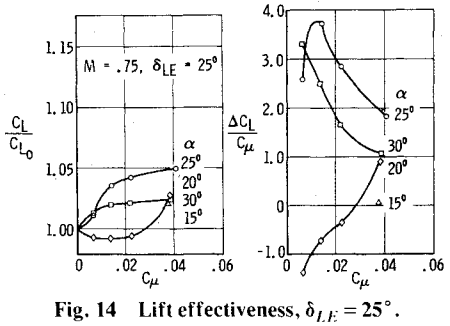

Fig. 14 Lift effectiveness, $\delta_{LE} = 25°$.

the flap shoulder, then the separated flow may be organized into an effective vortex system by blowing.

The life-effectiveness data for the leading-edge-flap deflected case are given in Figs. 13 and 14. Blowing is seen to be more effective at higher angles of attack for both leading-edge-flap cases. When the flap is deflected 25°, blowing is seen to be slightly detrimental to lift at an angle of attack of 20° and at the low C_μ values. It is pointed out that nozzle position studies were not made for low angles of attack with the leading-edge flap deflected 25°, since attached flow was expected to exist for these cases.

The incremental drag due to lift with leading-edge flaps deflected is summarized in Fig. 15. As in the case with no leading-edge flap deflection, Fig. 10, the drag due to lift is seen to be significantly lower than the flat-plate case, ΔC_L tanα. Thus, even with leading-edge flaps deflected, there is a measurable leading-edge thrust resulting from the augmented vortex flow over the upper surface of the wing.

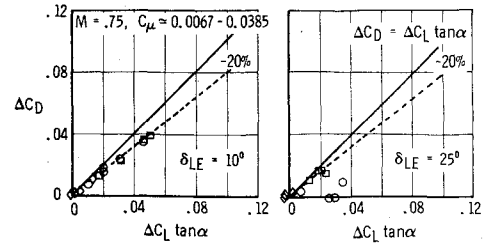

Fig. 15 Drag due to lift, $\delta_{LE} = 10°$ and 25°.

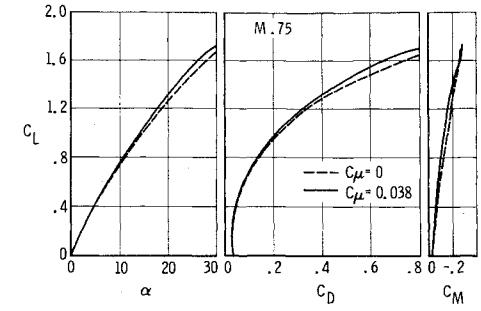

Fig. 16 Envelope force data.

Envelope Drag Polar

Current advanced fighter configurations designed for superior air combat capability employ the variable-camber concept in the transonic speed regime. The leading-edge flap is scheduled for deflection or is deflected manually, to assume its optimum position throughout the maneuver envelope. Thus the aircraft flies along an envelope drag polar representing the best polars for a given flight condition. Of course, envelope polars can be constructed which optimize lift or some other aerodynamic parameter. However, of most importance from a sustained maneuver standpoint is the polar, which has minimum drag for a given value of lift coefficient. It is of interest to compare the augmented-vortex force data with an envelope polar for the research configuration used.

The envelope polar for maximum lift-to-drag ratio over the C_L range is constructed for the present tests in Fig. 16. This figure shows the force envelopes for blowing-on and blowing-off at a Mach number of 0.75. An improvement in the aerodynamic characteristics is apparent. The data shown are not trimmed, but the horizontal tail is on. Inspection of the moment curves indicates that some further benefits in the form of reduced trim drag may accrue for the blowing concept when the aircraft is trimmed. The aerodynamic gains are not large for the blowing rates tested; however, the data show that favorable effects of vortex augmentation are possible. Of course the true measure of merit for this system depends upon the evaluation of the air supply source and thrust penalties that may be accrued by engine bleed.

Nozzle Position Studies

All of the data presented in the preceding sections were taken with the nozzle located at a position where the lift gains were greatest at the high blowing coefficients. As noted in the wind-tunnel test section, versatility in positioning the nozzle was obtained at some expense of precision in nozzle location. Thus, the results of the position studies should be considered more in the sense of trends with chordwise position and nozzle sweep angle than as precise optimum locators in these conceptual tests. The control of the vertical height of the nozzle was rather poor at high Mach numbers because of the deflection under load of the wing relative to the fixed nonmetric nozzle. Some lack of consistency in the blowing data at the high Mach number may result from variations in vertical height from run to run. In spite of the previous considerations, the data are satisfactory to accomplish the conceptual objectives of the test and give a clear indication of the importance of nozzle location for wing-leading-edge vortex

Table 2 Selected nozzle positions

δ_{LE}	α	$(x/c)_N$	Λ_N	C_L/C_{L0}
		$M=0.3, C_\mu \approx 0.17$		
0	10	0.3	30	1.111
	15	0.3	30	1.206
	20	0.3	40	1.359
	25	0.3	40	1.386
	30	0.4	40	1.283
		$M=0.75, C_\mu \approx 0.038$		
0	10	0.3	30	1.019
	15	0.3	30	1.119
	20	0.3	30	1.104
	25	0.3	30	1.093
	30	0.3	35	1.046
10	15	0.4	40	1.038
	20	0.4	40	1.010
	25	0.4	24	1.064
	30	0.18	40	1.053
25	20	0.4	25	1.027
	25	0.4	20	1.050
	30	0.4	40	1.025

enhancement. In order to conserve test time, position studies were not accomplished at angles of attack below 15°, since lift gains were expected to be small at the low angles of attack.

The nozzle positions selected for various configurations tested are summarized in Table 2. The better positions were selected on the basis of the ratio of the C_L-with-blowing to the C_L-without blowing. These values are shown in the table, along with the position data. For the low-speed-flow case ($M=0.3$), the variations in the lift with nozzle chordwise position and with sweep were relatively insensitive for positions aft of 30% chord. There was little difference in the lift generated for nozzle positions in the 30-40% chord range. In contrast, the higher Mach number data ($M=0.75$) without the leading-edge deflection reflect a clear optimum around the 30% chord position. A nozzle sweep of nominally 5° to 10° less than the leading-edge sweep of the wing was found to be favorable with the lading-edge flap undeflected. With the leading-edge flap deflected, the better chordwise position appeared to be further aft. This might be expected, since separation at the knee of the flap was felt to occur at higher angles of attack. Thus, the vortex system is generated further aft of the leading edge than when the leading-edge flap is not deflected. The nozzle position results provide trends for the various configurations tested. Further, the studies point out clearly that fine-tuning of the nozzle position may be an important factor for design of a fighter configuration that employs vortex augmentation by blowing.

Conclusions

The present conceptual test program has demonstrated that blowing vortex augmentation does result in significant improvement in lift and drag for a representative configuration with a cambered and twisted wing. The drag polar improvements result both from the increased vortex lift and from suction forces generated by the vortex flow over the cambered wing.

When the leading-edge flaps are deflected, the vortex augmentation provides gains in lift at angles of attack where the wing is influenced strongly by flow separations. The best wing performance may be achieved by combining vortex augmentation with small leading-edge-flap deflections to optimize the drag polar shape.

The effect of Mach number on the blowing effectiveness was found to be favorably up to at least $M=0.75$ in that generally greater lift increments for fixed C_μ were noted at the higher Mach number.

The overall blowing results are encouraging from an aerodynamic standpoint. Of course, the real potential for the blowing concept only can be evaluated considering the source of air for blowing, including the thrust penalties if engine bleed is used.

References

[1] Cornish, J.J., III, "High Lift Applications of Spanwise Blowing," ICAS Paper No. 70-09, Sept. 1970.

[2] Werle, H., "On Vortex Bursting," Office National d'Etudes et de Recherches, Chatillon, France, Note Technique No. 175, 1971.

[3] Bradley, R.G. and Wray, W.O., "A Conceptual Study of Leading Edge Vortex Enhancement by Blowing," *Journal of Aircraft,* Vol. 11, Jan. 1974, pp. 34-38.

[4] Polhamus, E.C., "Predictions of Vortex-Lift Characteristics by a Leading-Edge Suction Analogy," *Journal of Aircraft,* Vol. 8, April 1971, pp. 193-199.

[5] Dixon, J.G., Theisen, J.G., and Scruggs, R.M., "Theoretical and Experimental Investigations of Vortex Lift Control by Spanwise Blowing; Vol. I Experimental Research and Vol. II Three-Dimensional Theory for Vortex Lift Augmentation," Lockheed Georgia Company, Marietta, Ga., Rept. LG73ER-0169, Sept. 1973.

[6] Bradley, R.G., Smith, C.W., and Wray, W.O., "An Experimental Investigation of Lading-Edge Vortex Augmentation by Blowing," NASA CR-132415, April 1974.